

## Simple equation of state for solids under compression

Mercedes Taravillo, Valentín García Baonza, Javier Núñez, and Mercedes Cáceres

*Departamento de Química Física, Facultad de Ciencias Químicas, Universidad Complutense de Madrid, 28040 Madrid, Spain*

(Received 12 March 1996)

We recently proposed an isothermal equation of state that was successfully applied to study the high-pressure behavior of solids. Later, we developed a simple model to include temperature effects on the equation of state. In the present work we consider the prediction capabilities of the complete equation of state in the entire  $p$ - $V$ - $T$  surface of a solid. Our predictions have been compared with experimental data up to pressures of several GPa and temperatures between zero and temperatures rather higher than those of melting. We also compare the performance of our equation against the most successful equations of state proposed in the literature, with excellent results. The isothermal equation of state provides us an adequate representation of experimental pressure-volume data and a simple volume dependence for the Grüneisen parameter. The equation needs only four parameters evaluated at room pressure at a single reference temperature. [S0163-1829(96)03634-X]

### I. INTRODUCTION

In the past few decades, the equation of state (EOS) of a large number of solids has been studied up to rather high pressures and, in some cases, over a wide range of temperatures. The pressure dependence provides an extensive body of information on the nonlinear compressibility of solids and the temperature dependence reveals the effects of anharmonicity. A simple and accurate relation among the thermodynamic variables  $p$ ,  $V$ , and  $T$  that describes the EOS of a system, valid for all kind of solids, and reliable over the whole temperature and pressure ranges, is not yet available. In fact, most EOS are limited to temperatures well above the Debye temperature,  $\theta_D$ .

With regard to a pressure-volume relation that describes the compression of a solid, different approaches have been performed to derive semiempirical isothermal EOS.<sup>1-4</sup> Some authors<sup>1,4</sup> have used different linearization schemes to represent experimental  $pV$  data and so to obtain the isothermal EOS. Most of the resulting expressions depend on three zero-pressure parameters: the molar volume,  $V_0$ , the isothermal bulk modulus,  $B_0$ , and its isothermal pressure derivative,  $B'_0$ . One of the most successful isothermal EOS is that proposed by Vinet *et al.*<sup>1</sup> (hereafter referred to as MV2). This EOS is valid for all classes of solids in compression and in the absence of phase transitions. A successful isothermal EOS used for metallic solids is that proposed by Schulte and Holzapfel<sup>4</sup> [hereafter referred to as H11 (Ref. 5)]. This EOS depends only on two zero-pressure quantities:  $V_0$  and  $B_0$ , since they incorporate a correlation between  $B_0$  and  $B'_0$ . This represents a great improvement, because experimental values of  $B'_0$  are usually affected by large errors.<sup>4</sup>

In order to determine the complete EOS of a given solid from these relations, one needs to know the corresponding parameters at each temperature. Normally, polynomial expansions have been used to account for temperature dependence of these parameters. This procedure is limited by several reasons, but the most important besides increasing the number of needed parameters is the lack of extrapolation

capability of the resulting EOS.<sup>3</sup> Vinet *et al.*<sup>6</sup> tried to solve this problem by assuming that the thermal pressure is independent of the volume and linear with temperature above  $\theta_D$ , i.e., the quantity  $(\partial p/\partial T)_v$  is constant with the volume and the temperature. In this way, they showed how high-temperature properties may be predicted from a reference isotherm by introducing the zero-pressure value of the thermal (volumetric) expansion coefficient,  $\alpha_{p0}$ , as an additional parameter.<sup>6</sup> Nevertheless, we must bear in mind that the assumption of considering the quantity  $(\partial p/\partial T)_v$  as constant, is only approximate, and breaks down in the vicinity of, and below,  $\theta_D$ .<sup>7</sup> At absolute zero it vanishes, at low temperatures it increases rapidly and only above  $\theta_D$  remains almost constant. Therefore, the model proposed by these authors is formally valid only for temperatures above  $\theta_D$ . With regard to the H11 EOS, it only has been used as an isothermal relation. Temperature effects have not been analyzed yet.<sup>4</sup>

Recently, we have carried out a systematic analysis of the thermodynamic properties of a large number of solids. We first proved that there exists a simple universal isothermal EOS applicable to all condensed materials,<sup>8</sup> including solids. This universal function was derived from a pseudospinodal hypothesis. We subsequently studied the temperature dependence of the properties  $V_0$ ,  $B_0$ ,  $B'_0$ , and  $\alpha_{p0}$ , and we derived a simple model to predict these dependences from a pseudospinodal hypothesis using experimental results at a single reference temperature,  $T_{\text{ref}}$ .<sup>9</sup> The universal EOS is specified by the zero pressure values of  $V_0$ ,  $B_0$ ,  $B'_0$ , evaluated at  $T_{\text{ref}}$ , as well as an estimate of the Grüneisen parameter,  $\gamma^G$ , at this temperature, and the Einstein characteristic temperature,  $\theta_E$ . In our derivation it also is assumed that the thermal pressure is independent of the volume, however, the quantity  $(\partial p/\partial T)_v$  is not assumed to be constant with temperature; our method is therefore applicable over the whole temperature range. The success of our predictions in the temperature dependence of  $V_0$ ,  $B_0$ , and  $\alpha_{p0}$ , was tested using experimental data for typical solids such as xenon, sodium chloride, and gold.<sup>9</sup>

We will show that rather good accuracy can be obtained in our predictions when compared with experimental data for

a large number of different types of solids. The isothermal equation of state provide us an adequate representation of experimental pressure-volume data and a reasonable volume dependence for  $\gamma^G$ . We will also compare the complete universal EOS with two of the most successful EOS proposed in the literature, such as the model proposed by Vinet *et al.*<sup>6</sup> and H11 EOS referred to above.

The validity of the two isothermal EOS previously described does not imply that an EOS based on them must be successful over the whole  $p$ - $V$ - $T$  surface. In the present work, however, we shall demonstrate that a single reference thermodynamic state contains information enough to describe the complete EOS of the solid.

## II. UNIVERSAL EQUATION OF STATE

The basis of the universal equation is fully described in Ref. 9, so only its basic principles will be described here. The universal isothermal EOS which represents the pressure dependence of the molar volume can be written as<sup>8</sup>

$$V(p) = V_{sp} \exp\left\{-\frac{\kappa^*}{(1-\beta)} [p - p_{sp}]^{(1-\beta)}\right\}, \quad (1)$$

where  $V_{sp}$  and  $p_{sp}$  are the volume and the divergence pressure along a certain pseudospinodal curve (PSC), respectively, and  $\kappa^*$  and  $\beta$  are, respectively, an amplitude and the pseudocritical exponent that characterize the pressure behavior of the isothermal compressibility  $\kappa_T$  through the universal relation<sup>10</sup>

$$\kappa_T(p) = \kappa^* [p - p_{sp}]^{-\beta}, \quad (2)$$

$\beta$  being a universal constant close to 0.85. Although a detailed numerical analysis of this parameter shows that it changes slightly for different substances,<sup>11</sup> the value which will be used here, 0.85, is good enough for our purposes, as supported by our previous results.<sup>9</sup> We can obtain the parameters  $p_{sp}$ ,  $\kappa^*$ , and  $V_{sp}$  only from the zero-pressure quantities, namely,  $V_0$ ,  $B_0$ , and  $B'_0$ .<sup>8</sup>

One can obtain  $p(V, T)$  from Eq. (1) as follows. Assuming that  $\kappa^*$  and  $V_{sp}$  are both temperature independent (see Ref. 8), it is obtained that the thermal pressure is only temperature dependent, thus

$$p(V, T) - p(V, T_{ref}) = p_{sp}(T) - p_{sp}(T_{ref}). \quad (3)$$

From the Mie-Grüneisen equation,<sup>12</sup> we can obtain  $[p(V, T) - p(V, T_{ref})]$ , and assuming that the ratio  $(\gamma^G/V)$  is temperature independent, we have that  $p_{sp}(T)$  from Eq. (3) is

$$p_{sp}(T) = p_{sp}(T_{ref}) + \frac{\gamma^G(T_{ref})}{V(T_{ref})} [E_{vib}(T) - E_{vib}(T_{ref})], \quad (4)$$

where  $E_{vib}$  is the vibrational energy.

To obtain an analytic approximation to the EOS, we proposed the Einstein's expression for  $E_{vib}(T)$ , so the characteristic temperature,  $\theta_E$ , is required as an input parameter. It must be pointed out that, except at very low temperatures, no significant improvement is gained in our approach by using the Debye's theory.<sup>9</sup>

We must emphasize that the Mie-Grüneisen equation has been used here to obtain  $p_{sp}(T)$ , instead of using it to gen-

erate the thermal EOS of the solid. This procedure avoids some serious problems arising from the determination of the volume dependence of the ratio  $(\gamma^G/V)$ .<sup>13,14</sup> In addition, this procedure takes the advantage of introducing all the temperature dependences on the PSC, through  $E_{vib}$  in Eq. (4). Thus, provided  $E_{vib}(T)$  is known, the EOS of any solid can be determined from four experimental quantities only:  $V_0$ ,  $B_0$ ,  $B'_0$ , and  $\gamma^G$  evaluated at a single reference temperature,  $T_{ref}$ .

## III. RESULTS AND DISCUSSION

This section is divided as follows: first, we will show the application of Eq. (1) to represent pressure-volume data when it is compared with another isothermal EOS, such as MV2 EOS (Ref. 1) and H11 EOS.<sup>4</sup> Secondly, we will see that a simple volume dependence of  $\gamma^G$  is obtained from Eq. (1). Finally, we will further compare predictions obtained from our model with experimental data of the  $p$ - $V$ - $T$  surface and the thermal expansion coefficient of a solid.

Parameters required are listed in Table I for the solids studied in this work, along with selected reference temperatures and  $\theta_E$ . It must be pointed out that the values of  $B_0$  and  $B'_0$  for a given substance show considerable disagreement among different authors partly because they depend on the choice of the equation employed to describe the experimental data and on the range of pressure considered in the correlation, the values of  $B'_0$  are therefore commonly rather inaccurate, and, in general, there only exist reliable values of  $B'_0$  in the literature at room temperature. Thus, for ionic solids and metals, room temperature has been chosen as reference temperature. For some solids, we have used ultrasonic measurements, although they suffer from the same limitations as any other method of determining parameters.

Unlike others methods existing in literature, our treatment does not require experimental data at temperatures above or near  $\theta_D$ , where the quantity  $(\partial p/\partial T)_v$  varies only very weakly with temperature. Therefore, any temperature can be selected in our treatment. This feature is particularly useful for the study of solids with large values of  $\theta_D$ , since most experimental data are available at room temperature, which must be necessarily then selected as the reference temperature.

In Table II are recorded the zero-pressure values of the thermal expansion coefficient required to include temperature effects on the EOS according to the model of Vinet *et al.*<sup>6</sup>

### A. Application of Eq. (1) to represent pressure-volume data

An important feature of any universal EOS should be its ability to be put in a convenient reduced form that provides a principle of corresponding states and that suggests a convenient way of analyzing experimental data, as Vinet *et al.*<sup>1</sup> did. The basis of the isothermal MV2 EOS (Ref. 1) was a universal relation between the binding energy of the solid and intermolecular distance, from which these authors derived a universal function  $H(V)$  defined as

$$H(V) = \frac{(V/V_0)^{2/3}}{3[1 - (V/V_0)^{1/3}]} p(V). \quad (5)$$

TABLE I. Summary of the four input parameters as well as reference temperatures  $T_{\text{ref}}$  and Einstein temperatures  $\theta_E$  (calculated as  $0.75\theta_D$ , from the  $\theta_D$  values of the references) for the solids studied in this work. Parameters taken from Vinet *et al.* (Ref. 6) except where stated.

Substance	$T_{\text{ref}}$ (K)	$V_0$ (cm <sup>3</sup> mol <sup>-1</sup> )	$B_0$ (GPa)	$B'_0$	$\gamma^G$	$\theta_E$ (K)
Argon	40	23.026 <sup>a</sup>	2.35 <sup>a</sup>	7.5 <sup>a</sup>	2.7 <sup>b</sup>	69 <sup>c</sup>
Krypton	60	28.012 <sup>a</sup>	2.49 <sup>a</sup>	7.3 <sup>a</sup>	2.8 <sup>b</sup>	54 <sup>c</sup>
Xenon	60	35.54 <sup>a</sup>	3.02	7.8	2.8 <sup>b</sup>	48
Ice VII	300	12.3 <sup>d</sup>	23.9 <sup>d</sup>	4.2 <sup>d</sup>	1.2 <sup>d</sup>	1103 <sup>d</sup>
NaCl	298	27.00 <sup>e</sup>	23.5	5.35	1.59 <sup>f</sup>	240
LiF	300	9.833 <sup>e</sup>	66.4 <sup>e</sup>	5.23 <sup>e</sup>	1.63 <sup>e</sup>	551 <sup>g</sup>
NaF	300	15.02 <sup>e</sup>	46.1 <sup>e</sup>	5.28 <sup>e</sup>	1.52 <sup>e</sup>	367 <sup>g</sup>
CsCl	300	42.22 <sup>e</sup>	16.8 <sup>e</sup>	5.85 <sup>e</sup>	2.03 <sup>e</sup>	113 <sup>f</sup>
Au	300	10.21 <sup>h</sup>	166.65 <sup>i</sup>	5.4823 <sup>i</sup>	2.99 <sup>h</sup>	122
Cu	300	7.11 <sup>e</sup>	133.0 <sup>e</sup>	5.65 <sup>e</sup>	2.0 <sup>e</sup>	257 <sup>e</sup>

<sup>a</sup>Reference 18.

<sup>b</sup>Reference 45.

<sup>c</sup>Reference 46.

<sup>d</sup>Reference 26.

<sup>e</sup>Reference 47.

<sup>f</sup>Reference 16

<sup>g</sup>Reference 48.

<sup>h</sup>Reference 40.

<sup>i</sup>Reference 39

These authors tested the universality of  $H(V)$  for all classes of solids by evaluating  $H(V)$  using pressure-volume data of different classes of solids. From these values of  $H(V)$ , they plotted  $\ln H$  versus  $[1-(V/V_0)^{1/3}]$  and suggested for these plots a linear form of slope= $3/2(B'_0-1)$  and intercept= $\ln B_0$ . Thus  $\ln H$  was given as

$$\ln H(V) = \ln B_0 + 3/2(B'_0 - 1)[1 - (V/V_0)^{1/3}]. \quad (6)$$

From Eqs. (5) and (6) the isothermal MV2 EOS is obtained. However, if one in detail analyzes these plots of  $\ln H$  versus  $[1-(V/V_0)^{1/3}]$ , one can see that certain positive curvature exists for most solids, at least, at moderate compressions, as observed by Parsafar and Mason in organic solids.<sup>3</sup>

It can be confirmed that a similar expression to Eq. (6) is obtained from the isothermal H11 EOS, with an additional term:

$$\ln H(V) = \ln B_0 + C_{10}[1 - (V/V_0)^{1/3}] - \ln[(V/V_0)], \quad (7)$$

with  $C_{10} = -\ln(3B_0/p_{\text{FG0}})$ , where  $p_{\text{FG0}} = a_{\text{FG}}(Z/V_0)^{5/3}$ , with  $a_{\text{FG}} = 23.37 \text{ MPa nm}^5$ , represents the pressure of a free-

TABLE II. Summary of the values of  $\alpha_{p0}$  at the same reference temperatures than in Table I for the solids studied in this work. Parameters taken from Vinet *et al.* (Ref. 6) except where stated.

Substance	$10^4 \alpha_{p0}$ (K <sup>-1</sup> )
Argon	10.68 <sup>a</sup>
Krypton	9.04 <sup>b</sup>
Xenon	6.0
LiF	0.996 <sup>c</sup>
NaF	0.981 <sup>c</sup>
CsCl	1.41 <sup>d</sup>

<sup>a</sup>Reference 49.

<sup>b</sup>Reference 50.

<sup>c</sup>Reference 47.

<sup>d</sup>Reference 34.

electron gas (Fermi gas) with an electron density of  $Z$  electrons in the volume  $V_0$  for the solid at ambient conditions. Besides, H11 EOS yields a correlation between  $B_0$  and  $B'_0$ , due to the fact that  $B'_0$  is given as  $B'_0 = 3 + 2/3C_{10}$ . The additional terms of Eq. (7) incorporate a positive curvature that, at strong compressions, yield large deviations with respect to Eq. (6).

The function  $H(V)$  obtained from Eq. (1) is

$$H(V) = \frac{(V/V_0)^{2/3}}{3[1 - (V/V_0)^{1/3}]} \times \left[ p_{\text{sp}} + \left( \frac{(\beta-1)}{\kappa^*} \ln(V/V_{\text{sp}}) \right)^{1(1-\beta)} \right]. \quad (8)$$

A direct analysis of the Eq. (8) form is difficult to make, therefore, we will perform a numeric analysis for several solids.

Solid sodium chloride is interesting to study since it has been extensively used as pressure calibration standard.<sup>15</sup> Decker calculated the EOS for some ionic solids and estimated that their results contained a 1–2.4 % error in the pressure.<sup>16</sup> Their results for NaCl are those widely used as a pressure scale. We have evaluated  $\ln H$  for NaCl using pressure-volume data of Decker's model and we have fitted these results as function of  $[1-(V/V_0)^{1/3}]$  to Eq. (6) and to the expression resulting from Eq. (8). Comparing both fitting models it can be observed that the slight curvature exhibited by the data is better represented by our model. The differences in both fitting models can be seen if one plots the deviations obtained from both fits as illustrated in Fig. 1. Notice that the deviations from Eq. (6) imply, at least, a nearly parabolic form at these compressions.

We also have evaluated  $\ln H$  from experimental data of Mao *et al.*<sup>17</sup> up to 95 GPa for several metallic solids, namely, silver and copper. We have fitted these results against  $[1-(V/V_0)^{1/3}]$  to Eqs. (6) and (7) and to the expression resulting from Eq. (8). The differences obtained between the

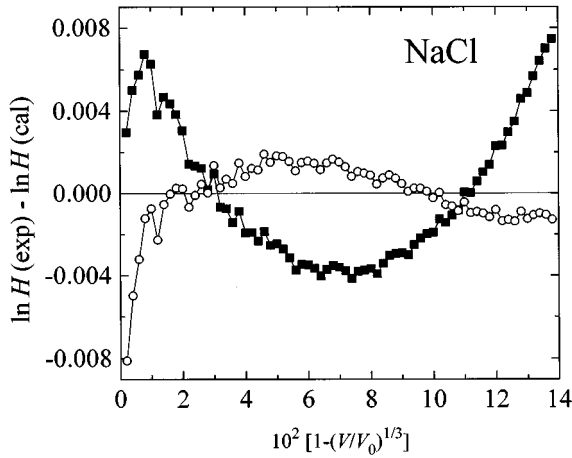


FIG. 1. Deviations between data of  $\ln H$ , where  $H(V)$  is a relation given by Eq. (5), and the values obtained from the different fitting models [ $\ln H(\text{cal})$ ], versus  $[1-(V/V_0)^{1/3}]$ , for solid NaCl (—○—), using Eq. (8); (—■—), using Eq. (6). Data are taken from Decker (Ref. 16).

experimental data and the different models are shown in Fig. 2. We see that our EOS yields always smaller deviations.

Figure 3 shows this sort of representation of the experimental data with data taken from Anderson and Swenson,<sup>18</sup> for solid krypton. Besides this, we have also shown the predictions obtained from the model proposed by Vinet *et al.*<sup>6</sup> and those obtained from Eq. (1) using as input data only those of zero pressure at 60 K. Once again it is observed that the experimental data have a certain curvature that is better captured by our model.

Finally, it must be noticed that the deviations in the  $\ln H$  plots has also been observed by Sikka for several metals.<sup>19</sup> This author has pointed out that one additional term in the expansion of Eq. (6) is adequate to account for these deviations. However, he considers that only in materials which undergo a rearrangement of electronic bands (e.g.,

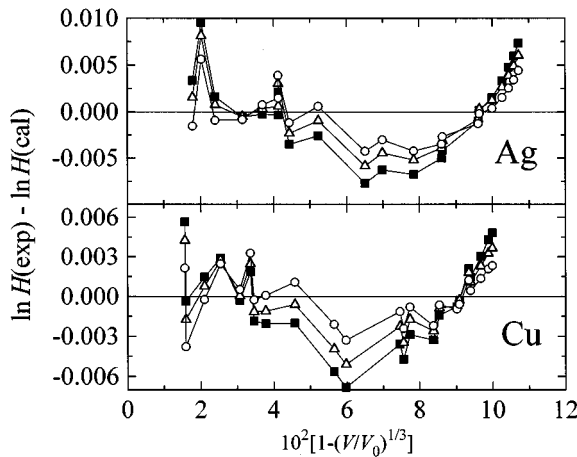


FIG. 2. Deviations between experimental values of  $\ln H$  and the values obtained from the different fitting models [ $\ln H(\text{cal})$ ], versus  $[1-(V/V_0)^{1/3}]$ , for solids silver and copper. (—○—), using Eq. (8); (—■—), using Eq. (6); (—△—), using Eq. (7). Experimental data are taken from Mao *et al.* (Ref. 17).

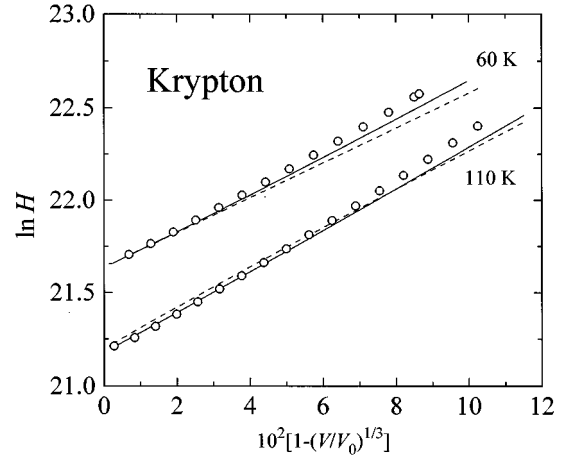


FIG. 3. Experimental values (○) of  $\ln H(V)$  versus  $[1-(V/V_0)^{1/3}]$ , for solid krypton, where  $H(V)$  is a relation given by Eq. (5). Data are taken from Anderson and Swenson (Ref. 18). Continuous lines, results calculated from our model by using the parameters recorded in Table I. Dashed lines, results calculated from the model proposed by Vinet *et al.* (Ref. 6).

*s*-electron-*d*-electron transition) as a function of compression additional terms must be taken into account.

### B. Volume dependence of the Grüneisen parameter $\gamma^G$

There are various ways of evaluating the Grüneisen parameter and it is normally assumed to be a function of volume only. A precise knowledge of the volume dependence of  $\gamma^G$  is essential for the full characterization of the EOS of a substance,<sup>13,20</sup> and various alternative formulations have been proposed for the volume dependence of  $\gamma^G$ . In this section we will analyze several approaches performed to derive this dependence.

A simple power dependence of  $\gamma^G$  on volume is widely used by most authors,<sup>21</sup> specifically

$$\gamma^G = \gamma_0^G (V/V_0)^q, \quad (9)$$

where  $\gamma_0^G$  is the zero-pressure value of  $\gamma^G$ , and  $q$  is a constant to be determined, and it can be calculated from thermodynamic quantities. It has been found that  $q$  is probably between 0.5 and 2 and has an uncertainty of as much as 0.7, for several ionic solids.<sup>21</sup> Therefore, the proposed value of  $q=1$ , assumed in the reduction of shock wave experiments to isothermal conditions, is within the error limits of this parameter. In this kind of experiments, it is assumed that  $C_V$  and  $(\partial p/\partial T)_V$  are both independent of the volume, and so  $q=1$ .<sup>13</sup>

This empirical result together with the fact that at very high compressions the limiting value for  $\gamma^G$  for all materials is  $2/3$  suggested the following interpolation formula for  $\gamma^G(V)$ ,<sup>13</sup>

$$\gamma^G = \gamma_0^G (V/V_0) + 2/3 [1 - (V/V_0)]. \quad (10)$$

More fundamental models suggested to calculate  $\gamma^G$  can be summarized by the following equations:<sup>13</sup>

$$\gamma^G(V) = -(2-t)/3 - \frac{V}{2} \frac{d^2(pV^{2t/3})}{dV^2} \bigg/ \frac{d(pV^{2t/3})}{dV}. \quad (11)$$

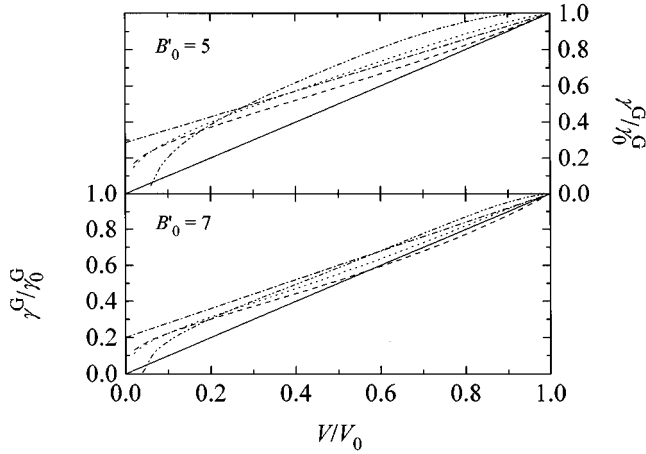


FIG. 4.  $(\gamma^G/\gamma_0^G)$  as function of  $(V/V_0)$  for two values of  $B'_0$ , 5 and 7 by using the Slater-Landau model to evaluate  $\gamma_0^G$ . Dashed lines calculated from Eq. (12). Continuous lines, calculated from Eq. (9) with  $q=1$ . Dash-dotted lines calculated from Eq. (10). Dotted and dash-double-dotted lines calculated from Eq. (11) with  $t=1$  and 2, respectively, by using the corresponding value of  $\gamma_0^G$  for each one.

The most popular values for  $t$  are  $t=0$  or 1 or 2, where the value  $t=0$  corresponds to the Slater-Landau model,<sup>13</sup> and the value of  $t=1$  was suggested by Dugdale and McDonald.<sup>22</sup> These models give almost equal values of  $\gamma^G$  as the pressure is increased and they differ mainly at low pressures.

As an example, we use the most widely used and simple model, namely, that of Slater-Landau, in order to determine the volume dependence of  $\gamma^G$  by using Eq. (1) to evaluate  $p$  and its derivatives. The expression obtained depends only on the reference values  $B'_0$  and  $V_0$ ,

$$\gamma^G(V) = -\frac{1}{6} + \frac{1}{2[(1/B'_0) + (1-\beta)/\beta \ln(V_0/V)]}. \quad (12)$$

The different relations between  $(\gamma^G/\gamma_0^G)$  and  $(V/V_0)$  are illustrated in Fig. 4 which includes the results obtained from Eq. (12), using two values of  $B'_0$  namely, 5 and 7, from Eq. (9), with  $q=1$ , and from Eq. (10). The Slater-Landau model is assumed in all cases. Within this model  $\gamma_0^G$  is given as  $\gamma_0^G = [3B'_0 - 1]/6$ . Notice that the relations obtained by Eq. (12) are found in good agreement with Eq. (9) at small compressions, where this model is usually applied, while that at large compressions Eq. (12) is closer to the limiting value imposed to Eq. (10).

We must be pointed out that there is an apparent inconsistency between the values obtained for  $\gamma_0^G$  by using the Slater-Landau model with experimental values of  $B'_0$ , and the values of  $\gamma_0^G$  obtained from thermodynamic quantities (see Table I). Except for gold, in all the cases, the latter values are smaller. If one uses other models [different values of  $t$  in Eq. (11)] to evaluate  $\gamma_0^G$  from  $B'_0$ , the following relation is obtained:

$$\gamma_0^G = [3B'_0 - 1 - 2t]/6. \quad (13)$$

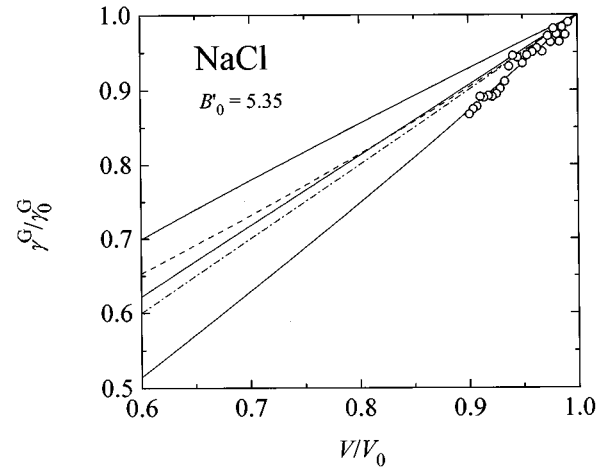


FIG. 5.  $(\gamma^G/\gamma_0^G)$  as function of  $(V/V_0)$  for NaCl. (○), experimental data taken from Boehler, Getting, and Kennedy (Ref. 23), reduced with their  $\gamma_0^G$  value. Continuous lines represent the results used and the band of uncertainty in  $(\gamma^G/\gamma_0^G)$  considered by Decker model (Ref. 16). Dashed line calculated from Eq. (12) by using  $B'_0$  of Table I for NaCl and the Slater-Landau model to evaluate  $\gamma_0^G$ . Dash-dotted line calculated from Eq. (9) with  $q=1$ .

According to Eq. (13) the values of  $t$  that correlate the values of  $B'_0$  and  $\gamma_0^G$  of Table I lie between 2 and 3, except for gold. Figure 4 shows the results of  $(\gamma^G/\gamma_0^G)$  as functions of  $(V/V_0)$  obtained from Eq. (11) with  $t=1$  and 2, by using Eq. (1) to evaluate  $p$  and its derivatives, and the corresponding value of  $\gamma_0^G$  for each one. However, there is notice that Eq. (1) does not give a good volume dependence of  $\gamma^G$  at low pressures in these cases. More recently, a generalization of Eq. (11) has been proposed where  $t$  is a characteristic parameter for each material.<sup>13</sup>

Boehler, Getting, and Kennedy<sup>23</sup> have determined the isothermal volume dependence of  $\gamma^G$  for NaCl using the most direct method possible, that is by measuring temperature increments during adiabatic compressions. Their results, reduced with their  $\gamma_0^G$  value, are shown as function of the compression in Fig. 5. This figure also contains the volume dependence of  $(\gamma^G/\gamma_0^G)$  used by Decker,<sup>16</sup> the band represents the uncertainty in  $(\gamma^G/\gamma_0^G)$  considered by Decker in fitting his EOS for NaCl. He obtained an exponent  $q$  of 0.93 (+0.37, -0.23). Volume dependence obtained from Eq. (12) by using  $B'_0$  of Table I for NaCl, and with Eq. (9) with  $q=1$  are also compared in Fig. 5. Both expressions lie between the band of uncertainty considered by Decker, and they are found in good agreement with the experimental data.

As already commented by Tallon,<sup>7</sup> the method used by Boehler, Getting, and Kennedy is markedly vulnerable to error in the pressure derivative of adiabatic bulk modulus and, as already pointed out, there are very few materials for which we have reliable and accurate values of this parameter. Tallon concluded that while  $q$  cannot be determined with any great exactitude, in all the cases considered by him, it was in the vicinity of unity, our model being consistent with this.

### C. Prediction of the $pVT$ surface

In this section we will show that the whole  $pVT$  surface of some solids can be easily and accurately predicted via the

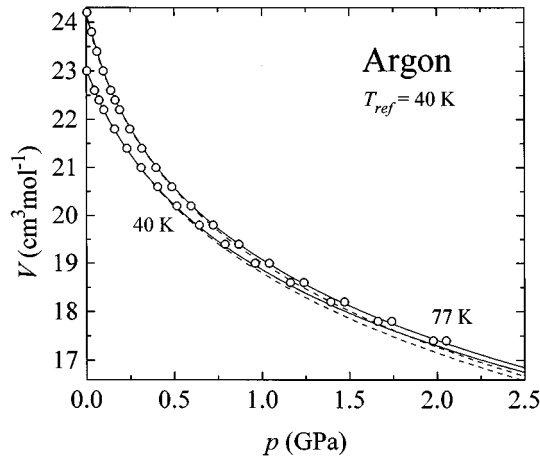


FIG. 6. Molar volume for solid argon at the following temperatures: 40 and 77 K. Experimental results (○) taken from Anderson and Swenson (Ref. 18). Continuous lines: results calculated from Eq. (1) using the parameters recorded in Table I. Dashed lines: results calculated from the model proposed by Vinet *et al.* (Ref. 6).

universal EOS [Eq. (1)] using a given set of zero-pressure data at a single reference temperature (Table I).

### 1. Rare gas and other molecular solids (ice VII)

The EOS for the rare gas solids argon, krypton, and xenon were determined by Anderson and Swenson<sup>18</sup> to 2 GPa at temperatures from 4.2 K to their triple point, by the piston-displacement technique. Due to the fact that these solids are highly compressible, relatively high values of the compression ( $V/V_0$ ) are reached in these experiments, although the range pressure is obviously small. In Fig. 6 we show their results for solid argon at 40 and 77 K. They are compared with the results obtained from Eq. (1) by using reference values at 40 K, and those obtained using the model proposed by Vinet *et al.*<sup>6</sup> The agreement between the predicted pressure-volume relations based on Eq. (1) and the experimental data is very good over a broad range of compressions.

The volumetric properties of solid argon were measured at room temperature by Ross *et al.*<sup>24</sup> up to 80 GPa using a diamond-window high-pressure cell. In an earlier work Bazonza, Cáceres, and Núñez<sup>8</sup> fitted their experimental data to Eq. (1) and they obtained the following characteristic parameters:  $V_{sp}=51.73 \text{ cm}^3 \text{ mol}^{-1}$ ,  $\kappa^*=0.144 \text{ GPa}^{-0.15}$ , and  $p_{sp}=0.28 \text{ GPa}$ . Notice that a positive value for  $p_{sp}$  is reasonable, since we are dealing with a temperature rather higher than that of its triple point (83 K) and so the solid phase at this temperature is stable for pressures higher than about 1.4 GPa.

We have determined the characteristic parameters for the same isotherm from our present model by taking reference data at 40 K. The results obtained are comparable to the previous values:  $V_{sp}=49.02 \text{ cm}^3 \text{ mol}^{-1}$ ,  $\kappa^*=0.138 \text{ GPa}^{-0.15}$ , and  $p_{sp}(298 \text{ K})=0.46 \text{ GPa}$ . The important feature is that our model is able to predict a larger value than zero too, although the reference is taken from the region of large negative pseudospinodal pressures. The prediction obtained from Eq. (1) is plotted in Fig. 7 up to 700 GPa, where it is compared with the results obtained by Ross *et al.*<sup>24</sup> from Monte Carlo calculations for solid argon using an (exp-6)

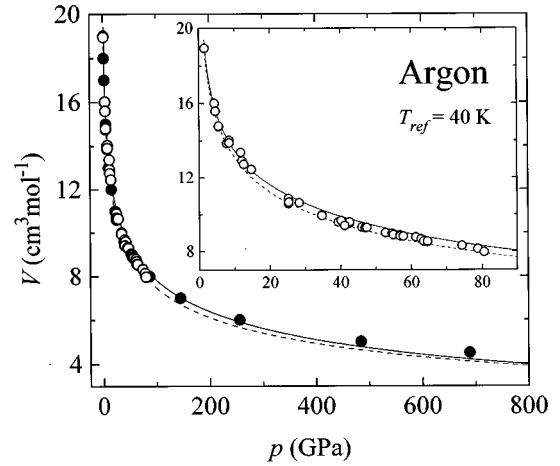


FIG. 7. Continuous line: molar volume results calculated from Eq. (1) using zero-pressure data at 40 K as input (Table I) for solid argon. (○): experimental results at room temperature reported by Ross *et al.* (Ref. 24) (see inserted figure) and (●), those calculated by them from Monte Carlo calculations using an (exp-6) potential. Dashed line calculated from the model proposed by Vinet *et al.* (Ref. 6).

potential. A good agreement is found between sets of data at the highest pressures. Notice that Fig. 7 of the present work is similar to Fig. 7 of Ref. 8. However, we must emphasize that while our previous results were obtained by the fit of experimental data up to 80 GPa to Eq. (1), we actually perform a prediction at room temperature using zero-pressure values at 40 K.

In Fig. 8 the prediction obtained from Eq. (1) by using zero-pressure values at 60 K (Table I) for solid krypton is shown for two temperatures. A good agreement is found again with experimental data of Anderson and Swenson.<sup>18</sup>

Finally, results obtained for solid xenon are very good also. Figure 9 compares experimental data taken from

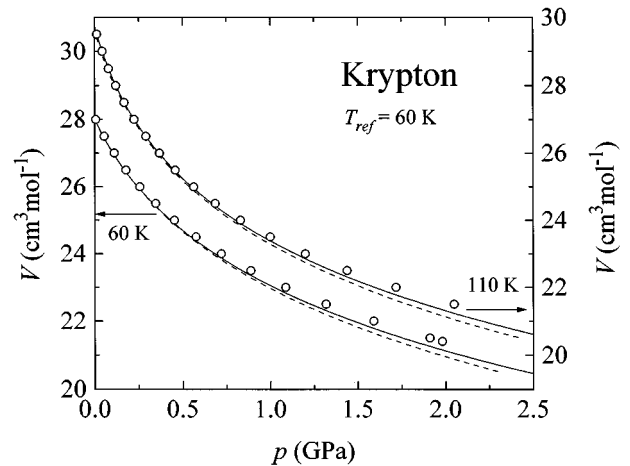


FIG. 8. Molar volume for solid krypton at the following temperatures: 60 and 110 K. Experimental results (○) taken from Anderson and Swenson (Ref. 18). Continuous lines, results calculated from Eq. (1) using the parameters recorded in Table I. Dashed lines, results calculated from the model proposed by Vinet *et al.* (Ref. 6). Notice that the left and right axis are referred to 60 and 110 K, respectively.

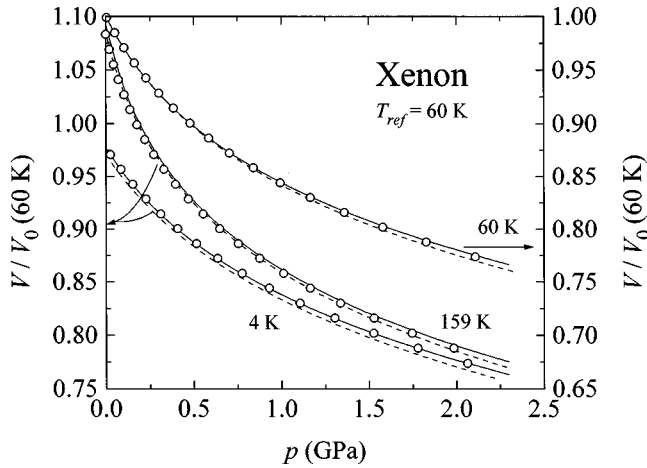


FIG. 9. Relative compressions of solid xenon at the following temperatures: 4, 60, and 159 K. Experimental data (○) taken from Anderson and Swenson (Ref. 18). Continuous lines, results calculated from Eq. (1) using the parameters recorded in Table I. Dashed lines, results obtained from the model proposed by Vinet *et al.* (Ref. 6). Notice that the left axis is referred to 4 and 159 K and the right one to 60 K.

Anderson and Swenson<sup>18</sup> with those calculated from Eq. (1) by using zero-pressure values at 60 K. To compare our model and that proposed by Vinet *et al.*<sup>6</sup> directly, we have used the reference values taken by them. The prediction based on Eq. (1) is in good agreement with experimental data, even at temperatures below  $\theta_D$ . Although the model proposed by Vinet *et al.*<sup>6</sup> is only valid for temperatures above  $\theta_D$ , we have compared both models for the isotherm of 4 K and it can be observed a systematic deviation between both models over the whole compression range. This is due to the fact that the isothermal MV2 EOS predicts correctly the pressure behavior, but the EOS of Vinet *et al.*<sup>6</sup> underestimates  $V_0$  for temperatures below  $\theta_D$ . This is not of great significance in  $V/V_0$  but the effect in the prediction of properties such as  $\alpha_p$  is quite important, as it will be discussed in Sec. III D.

Solid ice VII is the stable high-pressure phase at room temperature above 2.3 GPa; no phase change has been observed up to 128 GPa.<sup>25</sup> Fei, Mao, and Hemley<sup>26</sup> measured the volumetric properties of ice VII from 3 to 20 GPa and 300–650 K using a diamond anvil cell. The uncertainty in measured pressure is of  $\pm 0.2$ –0.3 GPa. These authors fitted their  $pV$  data at room temperature and obtained the parameters  $V_0$ ,  $B_0$ , and  $B'_0$ . In order to determine high-temperature properties, they used the following expression to represent  $\alpha_p$ :

$$\alpha_p(p, T) = \alpha_{p0}(T) [1 + (B'_0/B_0)p]^{-\eta}, \quad (14)$$

where  $\alpha_{p0}(T)$  is the zero-pressure thermal expansion coefficient, which is expressed as a linear function of temperature, and  $\eta$  is an adjustable parameter. Fitting their  $pVT$  data, they found a parameter set that reproduced the experimental data with a standard deviation of  $\pm 0.02$  cm<sup>3</sup> mol<sup>-1</sup>. In addition, the  $pVT$  data were also fitted with a Mie-Grüneisen relation,

TABLE III. Comparison of  $pVT$  data of ice VII. (a) Experimental results taken from Fei, Mao, and Hemley (Ref. 26). (b) Predictions calculated from our method with the parameters recorded in Table I.

$T$ (K)	$p$ (GPa)	$V$ (cm <sup>3</sup> mol <sup>-1</sup> )	
		(a)	(b)
350	6.00	10.36(1)	10.37
	14.11	9.03(1)	9.07
	17.80	8.64(2)	8.67
400	6.55	10.27(2)	10.29
	13.85	9.09(2)	9.12
	15.44	8.89(2)	8.94
450	6.57	10.33(2)	10.34
	12.88	9.27(2)	9.27
	15.03	8.96(2)	9.01
	18.67	8.60(3)	8.62
500	6.52	10.40(2)	10.40
	12.28	9.38(3)	9.39
	17.90	8.71(2)	8.72
550	6.50	10.51(1)	10.46
	11.70	9.53(2)	9.51
	17.39	8.80(1)	8.80
600	11.17	9.68(2)	9.63
	17.00	8.92(1)	8.87
650	15.95	9.15(2)	9.02

in which  $\gamma^G$  was assumed to be a function only of volume according to Eq. (9), that allowed them to obtain the values of  $\gamma_0^G$  and  $\theta_D$ .

We have calculated the volume of ice VII from our method, by using zero-pressure values at 300 K, obtained by Fei, Mao, and Hemley<sup>26</sup> from their different fits. The results are recorded in Table III together with their experimental data. The agreement between our predictions and the experimental data is reasonable taking into account the experimental uncertainty, and comparable with that obtained by them from their fit to the relation of  $\alpha_p$ .

## 2. Ionic solids

We shall now show the validity of our approach to predict the relative compressions of several ionic solids. Boehler and Kennedy<sup>27</sup> reported accurate compression data of solid NaCl up to 3.2 GPa and 773 K using a piston cylinder apparatus in which the length change of a single crystal of this substance is determined. They estimated an accuracy in  $\Delta V/V_0$  of 0.7%. Figure 10 shows the comparison of the experimental relative compressions reported in Ref. 27 with those predicted from Eq. (1). Results of Decker model<sup>16</sup> for NaCl, already used in Sec. III A, are also shown in Fig. 10. We find a good agreement between our predictions and the experimental data over the entire range of temperatures. Notice that our compressions are a little smaller than those given by the Decker model. However, there are debates<sup>27–29</sup> on the accuracy of semiempirical Decker's EOS which is used as pressure calibration. Especially at high temperatures, there is no experimental verification for his NaCl scale. One of the difficulties with Decker's EOS is that it yields a theoretical

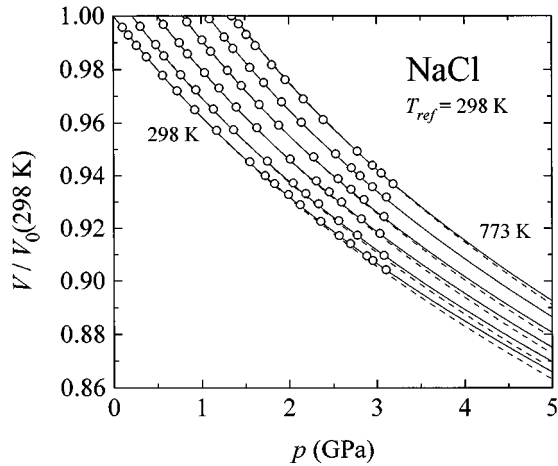


FIG. 10. Continuous lines represent the prediction of relative compressions for solid NaCl calculated from Eq. (1) using as input the parameters recorded in Table I (○), experimental data from Boehler and Kennedy (Ref. 27) plotted at the following temperatures: 298, 373, 473, 573, 673, and 773 K. Dashed lines, results from the Decker model (Ref. 16).

value of 4.93 for  $B'_0$ , when ultrasonic measurements yield a value of 5.35, value used here by us. Up to its transition pressure to the CsCl structure at about 29 GPa,<sup>21</sup> the NaCl scale appears to be reliable, although there are small discrepancies between the NaCl and CsCl scales up to 3 GPa (Ref. 30) and more serious discrepancies up to 30 GPa.<sup>31</sup>

Results for other ionic solids such as LiF, NaF, and CsCl, are summarized in Figs. 11–13. Compressibility of these solids at room temperature was measured by Drickamer and co-workers<sup>32,33</sup> by x-ray-diffraction techniques. Boehler and Kennedy<sup>29</sup> also reported accurate compression data for solid LiF up to 3.2 GPa and 673 K, by using the same method as in Ref. 27. However, the only experimental determination of relative compressions, which is extended over a wide temperature range (up to 1073 K), is the work reported by

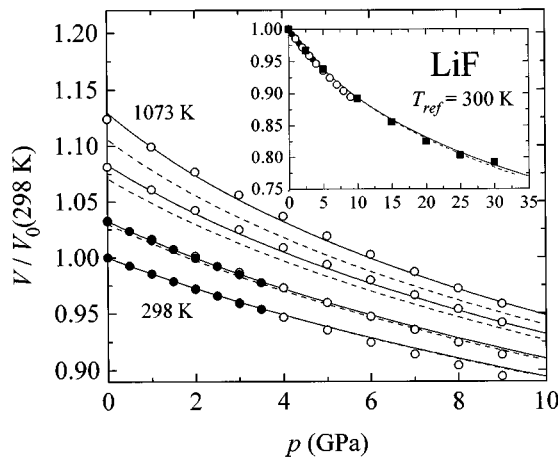


FIG. 11. Relative compressions for solid LiF at the following temperatures: 298 (see inserted figure), 573, 673, and 1073 K. Experimental sources (●) Boehler and Kennedy (Ref. 29); (■), Pagannone and Drickamer (Ref. 32), and (○), Yagi (Ref. 34). Continuous lines calculated from Eq. (1) with the parameters recorded in Table I. Dashed lines calculated from the model proposed by Vinet *et al.* (Ref. 6).

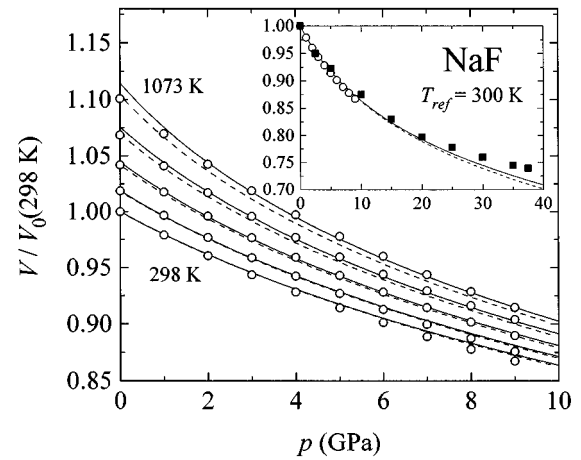


FIG. 12. Relative compressions for solid NaF at the following temperatures: 298 (see inserted figure), 473, 673, 873, and 1073 K. Experimental sources: (■), Pagannone and Drickamer (Ref. 32) and (○), Yagi (Ref. 34). Continuous lines calculated from Eq. (1) with the parameters recorded in Table I. Dashed lines calculated from the model proposed by Vinet *et al.* (Ref. 6).

Yagi.<sup>34</sup> We will also compare the results obtained from the model proposed by Vinet *et al.*<sup>6</sup> for the three alkali halides. We will compare the results reported by Yagi with our predictions, since, to the best of our knowledge, no other experimental data do exist at the highest temperatures. We must point out however, that a comparison of our predictions with other experimental data from literature reveals that Yagi's results have some systematic deviations at the highest pressures.

Figure 11 (see inserted figure) shows the comparison of the experimental relative compression<sup>29,32,34</sup> at room temperature with that predicted from Eq. (1) for solid LiF. Our

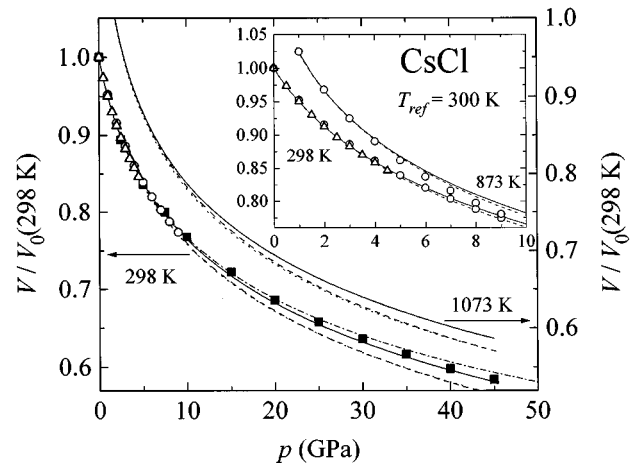


FIG. 13. Pressure dependence of relative compressions for solid CsCl at the following temperatures: 298, 873 (see inserted figure), and 1073 K. Experimental sources: (■), Perez-Albuerne and Drickamer (Ref. 33); (○), Yagi (Ref. 34); and (△), Vaidya and Kennedy (Ref. 35). Continuous lines, prediction of Eq. (1) using zero-pressure data as input (Table I). Results calculated from the model proposed by Vinet *et al.* (Ref. 6) (dashed lines) are indistinguishable from those calculated from the Decker model (Ref. 16) (dotted lines). Dash-dotted line, extrapolated ultrasonic equation taken from Barsch and Chang (Ref. 36).



predictions for higher temperatures, up to 1073 K, are also compared in Fig. 11. The agreement with experimental data is good over the whole compression range. Similar results are compared in Fig. 12 for solid NaF.

Figure 13 compares the relative compressions calculated from our method by using zero-pressure values at 300 K, for solid CsCl at the following temperatures: 298, 873, and 1073 K, with experimental data.<sup>33–35</sup> We found excellent agreement with the results of Perez-Albuerna and Drickamer.<sup>33</sup> In Fig. 13 it can be seen that the Decker<sup>16</sup> model for CsCl and that proposed by Vinet *et al.*<sup>6</sup> yield quite similar results, although both models give lower pressures than those obtained from an extrapolated Birch second-order empirical equation proposed by Barsch and Chang<sup>36</sup> for CsCl, where the three parameters were ultrasonically measured. That expression was compared by Decker and Worlton.<sup>30</sup> These authors measured the compression of NaCl and CsCl to 3.2 GPa using time-of-flight neutron diffraction techniques. They compared their results for CsCl with that ultrasonic equation, and comparing the Decker<sup>16</sup> model and this equation, they indicated that the Decker model yielded a slightly lower pressure than the ultrasonic equation and they suggested that if one should use CsCl as a pressure calibrant they should increase the pressure calculated by Decker's EOS by about 2% for pressures up to 3 GPa.<sup>30</sup> Their conclusion is also consistent with our predictions for CsCl and confirms our previous discussion on NaCl.

### 3. Metallic solids

Finally, we will compare some results obtained for metallic solids. In the past decade, ultrahigh pressure research is at the stage that a calibration standard is needed for experiments at high temperatures and pressures. Among the two most common methods of pressure calibration are the use of an internal standard (e.g., NaCl, as discussed above) or the ruby-fluorescence pressure scale.<sup>15</sup> More recently, metals such as gold<sup>26</sup> and platinum<sup>37</sup> have been used and proposed as internal calibration standards. Therefore, it is important to dispose an accurate EOS up to ultrahigh pressure. At the same time, the study of the physics of metals at ultrahigh pressure is also of considerable current interest, since these extreme pressures can lead to significant changes in atomic, electronic, and chemical structure.<sup>38</sup>

Heinz and Jeanloz<sup>39</sup> measured the compression of solid gold at room temperature to 70 GPa using a diamond anvil cell and derived a thermal EOS for solid gold using a Mie-Grüneisen-like equation. They estimated that their results contained 1–2 % error in the pressure. As we have already commented a problem arises from uncertainties in the value of  $B'_0(T_{\text{ref}})$ , extrapolations from high-pressure measurements usually give lower values than those obtained from ultrasonic measurements.<sup>37</sup> In their analysis of experimental data, Heinz and Jeanloz found a value close to 5.5 for this quantity, while the most ultrasonic measurements give values around 6.5.

Another EOS for gold was derived by Anderson, Isaak, and Yamamoto.<sup>40</sup> They introduced an anharmonic volume correction to the thermal pressure, and calculated  $p(V, T)$  by using the same values of  $B_0$  and  $B'_0$  of Heinz and Jeanloz.

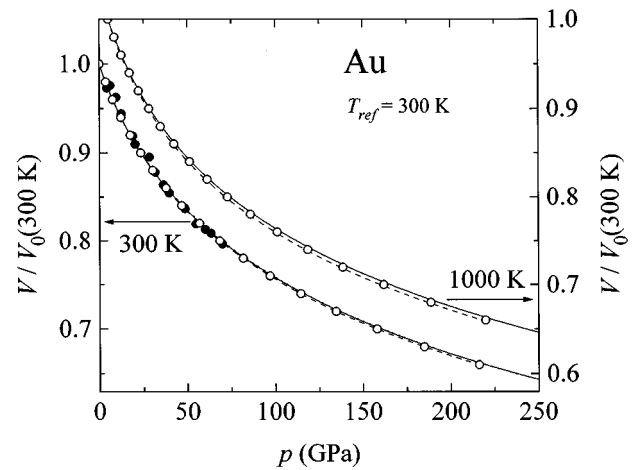


FIG. 14. Relative compressions for solid gold at the following temperatures: 300 and 1000 K. (●), experimental results, and (○), estimations taken from Heinz and Jeanloz (Ref. 39); dashed lines estimations of Anderson, Isaak, and Yamamoto (Ref. 40) using the anharmonic correction. Continuous lines prediction calculated from Eq. (1). Prediction from H11 EOS (Ref. 4) at room temperature is indistinguishable from our model. Notice that the left and right axis are referred to 300 and 1000 K, respectively.

We have estimated high temperature isotherms near the melting point from Eq. (1) by using these same input data at 300 K (Table I).

Figure 14 compares our predictions for gold with the experimental data and estimates of Heinz and Jeanloz,<sup>39</sup> and the estimates of Anderson, Isaak, and Yamamoto.<sup>40</sup> Excellent agreement is found with our model over the entire range of compression. It must be pointed out that, at 300 K, our EOS is indistinguishable from the H11 EOS. This means that both models should yield very similar results at any temperature. However, since experimental results required for the H11 are not available, numerical calculations cannot be performed. One can always include our predicted results into the H11 equation, but this procedure does not provide any relevant information right now. This is, however, a suggestive alternative to introduce temperature effects into the H11 as will be commented in future paragraphs. With regard to the value of  $B'_0$ , from the H11 EOS and with the values of  $V_0$  and  $B_0$  of Table I, it is obtained a value of 5.74 for  $B'_0$ , that it is a little higher than that found by Heinz and Jeanloz,<sup>39</sup> and smaller than that ultrasonic one.

Figure 15 shows the relative compression at room temperature for solid copper. The prediction based on Eq. (1) is compared with experimental data up to 95 GPa taken from Mao *et al.*<sup>17</sup> Also illustrated in Fig. 15 is the same isotherm for copper as calculated in the 100–1000 GPa pressure range and suggested as a possible pressure calibration standard by Nellis *et al.*<sup>38</sup> These authors give a  $\pm 10\%$  as upper-bound estimate on the uncertainty in their calculated pressures. Corresponding pressure-volume relation calculated from H11 EOS is also shown in Fig. 15. H11 EOS yields a value of 5.18 for  $B'_0$ , that it is a little smaller than that obtained from ultrasonic measurements used by us (Table I). The overall agreement between the different EOS and experiment data is good and within estimated error.

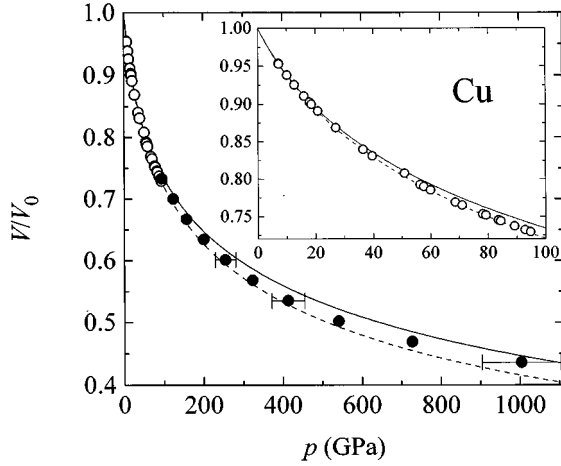


FIG. 15. Relative compression at room temperature for solid copper. (○), experimental data taken from Mao *et al.* (Ref. 17); (●), results calculated by Nellis *et al.* (Ref. 38). Continuous lines calculated from Eq. (1). Dashed lines calculated from H11 EOS (Ref. 4).

#### D. Prediction of thermal expansion coefficient at high pressures

Experimental measurements of thermal expansion at high pressures have been limited. A direct determination is that used by Fuchs, Pruzan, and Ter Minassian<sup>41</sup> by means of a calorimetric method. Furthermore, the thermal expansion can be determined from precise volume data available over a broad temperature range. In most cases, however, this kind of measurements is limited to atmospheric pressure. On the other hand, when  $pVT$  measurements at high pressure are available, their accuracy is normally insufficient to reliably predict the thermal expansion. Therefore, an accurate method to predict its pressure behavior is of great interest.

For molecular liquids, it has been found that the pressure behavior of  $\alpha_p$  is well represented by a power law identical in form to Eq. (2), but with a pseudocritical exponent,  $\beta$ , close to 0.5 instead of close to 0.85 as found for  $\kappa_T$ .<sup>42</sup> This treatment was also applicable to solids, but  $\beta$  is equal to 0.85, as in the case of  $\kappa_T$ , as already was pointed by us.<sup>8</sup>

The following expression for  $\alpha_p$  can be derived from Eq. (1),

$$\alpha_p(p, T) = \frac{1}{V_{sp}} \frac{dV_{sp}}{dT} - \frac{d\kappa^*}{dT} \frac{[p - p_{sp}]^{(1-\beta)}}{(1-\beta)} + \frac{dp_{sp}}{dT} \kappa^* [p - p_{sp}]^{-\beta}. \quad (15)$$

If now we assume that  $\kappa^*$  and  $V_{sp}$  are temperature independent, following our model,  $\kappa_T$  and  $\alpha_p$  are represented by similar expressions with equal exponents, and therefore the quantity  $(\partial p / \partial T)_v$  is given by the derivative of PSC,

$$\alpha_p(p, T) = \frac{dp_{sp}}{dT} \kappa^* [p - p_{sp}(T)]^{-\beta}. \quad (16a)$$

It follows from Eq. (16a) that  $\alpha_{p0}$  can be calculated as  $\alpha_{p0} = (dp_{sp}/dT)/B_0$ . If one identifies the different terms (am-

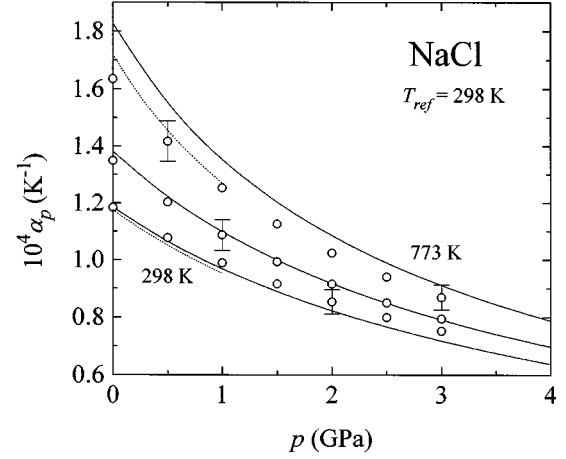


FIG. 16. Pressure dependence of the thermal (volumetric) expansion coefficient for solid NaCl at the following temperatures: 298, 473, and 773 K. (○), results obtained from Boehler and Kennedy (Ref. 27). Continuous lines calculated from Eq. (1). Dotted lines, results from ultrasonic measurements by Spetzler, Sammis, and O'Connell (Ref. 43) at 300 and 800 K.

plitude and the divergence pressure) with the values of  $\alpha_{p0}$ ,  $B_0$ , and  $B'_0$ , the following expression is obtained

$$\alpha_p(p, T) = \alpha_{p0}(T) [1 + (B'_0(T)/\beta B_0(T))p]^{-\beta}. \quad (16b)$$

It can be observed that Eq. (14) used by Fei, Mao, and Hemley<sup>26</sup> to represent  $\alpha_p$  of ice VII is quite similar to Eq. (16b), although it presents several differences. The first difference is that they used an empirical function of temperature for  $\alpha_{p0}$ , while a universal function (given by the PSC and its derivative) arises in a natural way from our model, which is expected to be valid over the whole temperature range. Notice also that  $\theta_D$  obtained by Fei, Mao, and Hemley is quite higher than room temperature and therefore the linear function for  $\alpha_{p0}$  obtained by them is too stiff yielding too large values of  $\alpha_{p0}$  at high temperatures. Another difference is that while in Eq. (14) the parameters  $B_0$  and  $B'_0$  are those obtained at room temperature, within our model, these values depend on the temperature, so different divergence pressures are derived from each one, as we already have pointed out.<sup>8</sup> Instead, these authors found  $\eta$  to be 0.9 for ice VII, a value quite close to  $\beta$  value. However, we believe that neither the  $pVT$  data grid (see Table III) is sufficiently dense, nor the accuracy of their measurements is high enough to predict the thermal expansion with reasonable accuracy.

In a work of Boehler and Kennedy,<sup>27</sup> accurate volume measurements for solid NaCl allowed them to determine the thermal expansion up to 3 GPa and 773 K. These authors fitted their experimental  $pV$  data to a modified Murnaghan equation and used thermal expansion data to extrapolate their compression curves to atmospheric pressure. Volume data were calculated from the smoothed curve by integration of Murnaghan equation. From these volume data they calculated the volume coefficients of thermal expansion and they found that  $\alpha_p$  is essentially a linear function of temperature, and that the quantity  $(\partial p / \partial T)_v$  remains nearly constant over a large pressure and temperature range. Recall that this assumption was used by Vinet *et al.*<sup>6</sup> for temperatures above

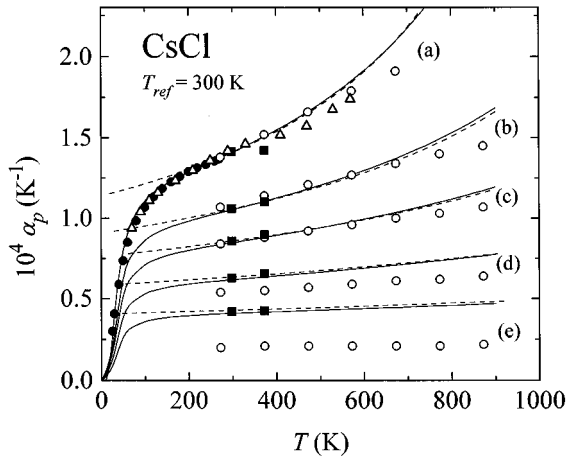


FIG. 17. Thermal (volumetric) expansion coefficient of solid CsCl as function of temperature along five isobars:  $p$ =(a) 0, (b) 1, (c) 2, (d) 4, and (e) 8 GPa. Experimental sources: (●), zero-pressure data taken from Bailey and Yates (Ref. 51); (△), zero-pressure data taken from Rapp and Merchant (Ref. 52); (○), Yagi (Ref. 34); and (■), Bijanki and Hardy (Ref. 44). Continuous lines calculated from Eq. (1) using zero-pressure data as input. Dashed lines calculated from the model proposed by Vinet *et al.* (Ref. 6).

$\theta_p$ . Figure 16 shows the pressure dependence of the thermal expansion at several temperatures: 298, 473, and 773 K, obtained by Boehler and Kennedy. The error bars indicate an error of a 5% in  $\alpha_p$ . Results obtained from ultrasonic measurements by Spetzler, Sammis, and O'Connell<sup>43</sup> at 300 and 800 K are also illustrated. These results are compared with our predictions using only zero-pressure values at 298 K. The discrepancies at higher temperatures can be attributed to thermal expansion data greater than those used by Boehler and Kennedy for the extrapolation commented above, as already was pointed out by Tallon.<sup>7</sup> In spite of this, the pressure behavior predicted for thermal expansion is remarkably good.

High pressure thermal expansion for solid CsCl has been also calculated from our model by using zero-pressure values at 300 K. This quantity is plotted in Fig. 17 as function of temperature along several isobars. The agreement is very good with the quasiharmonic model of Bijanki and Hardy.<sup>44</sup> Good agreement is found with the values calculated from the model proposed by Vinet *et al.*,<sup>6</sup> in the temperature range where their relation holds. Calculated values from isothermal compression curves by Yagi<sup>34</sup> are also shown. At the highest pressures (4 and 8 GPa) it can be observed that their results are smaller than our predictions and those of Vinet *et al.* This confirms that their results seem to show excessively large relative compressions, as commented above.

#### IV. CONCLUSION

Regarding to the  $H$  quantity, we have confirmed that can be represented by a universal form, as already was pointed out by Vinet *et al.*<sup>1</sup> We have proved, however, that the plots of  $\ln H$  versus  $[1-(V/V_0)^{1/3}]$  obtained from experimental data present a certain curvature. In terms of extrapolation capabilities at very high compressions we believe that care must be taken in using any EOS based on a linear dependence of  $\ln H$ . The expression associated to the H11 EOS

incorporates some improvement. However, we have found that best results are obtained when Eq. (8) is used to account for  $H$ .

It has been of interest to see what Eq. (1) predicts about the behavior of  $\gamma^G$ . Due to the relative inaccuracy on the determination of  $\gamma^G$  as a function of volume, we have confirmed that Eq. (1) yields a reasonable description of the general volume dependence of this property according to Slater-Landau model. Equation (12) yields a simple and physically reasonable volume dependence of  $\gamma^G$  and is a well-behaved expression over the whole range of compressions.

This represents an indirect confirmation of the assumptions included in our model to account for the temperature dependence of PSC. If the parameters  $\kappa^*$  and  $V_{sp}$  are both temperature independent, the thermal pressure is only temperature dependent, and  $C_V$  and  $(\partial p/\partial T)_v$  are both independent of the volume, so  $\gamma^G$  is represented by Eq. (9) with  $q=1$ .

The main goal of our model is that only four zero-pressure parameters evaluated at a single temperature and  $\theta_E$  suffice to predict high-pressure isotherms at any temperature. This issue has a tremendous importance in high pressure research when results at different temperatures are required, since usually only the room temperature isotherm is experimentally known. As we have shown in this work, our model predicts high pressure  $pV$  isotherms at very low temperatures and at temperatures as high as those of melting and above. Besides this, the characteristic parameters preserve their physical significance (see, for instance, the results of solid argon at room temperature). Another important feature of our model is that it predicts the pressure behavior of the thermal expansion coefficient over the whole temperature range without including any additional assumptions or experimental information.

Let us summarize the most important improvements gained with our  $pVT$  EOS when it is compared with others considered as successful in the literature. Our model is of a quality comparable to those of Vinet *et al.*<sup>6</sup> and Holzapfel (H11 isothermal EOS) for the estimation of the  $pVT$  behavior at medium high densities. However, according to the approximation of considering a linear form to represent  $\ln H$  as function of  $[1-(V/V_0)^{1/3}]$ , it is observed that the EOS of Vinet *et al.* usually yields compressions larger than our isothermal EOS. With regard to the prediction of the thermal expansion coefficient at high pressure, we corroborate the improvement gained with our model, which is valid over the whole temperature range. The prediction and extrapolation capabilities of Eq. (1) are comparable to those of the isothermal H11 EOS (for metals). However, a considerable improvement of our model is the simple procedure of introducing the temperature dependence on the EOS through that of the PSC. We are already considering the possibility of using this procedure to introduce the temperature dependence on other EOS, such as the H11 one. This would confirm the general validity of considering the PSC as a natural way of including the temperature dependence on the EOS; this feature would be particularly useful in analyzing results obtained from shock wave measurements.

Finally, it is interesting to point out that one can estimate the pseudocritical exponent  $\beta$  from H11 EOS model using

the relation that correlates  $p_{sp}$  with  $B_0$  and  $B'_0$  ( $p_{sp} = -\beta B_0/B'_0$ ). The resulting values of  $\beta$  are slightly smaller than ours (ca. 0.72, in average, about 70 metals). If  $\beta$  is computed from the relation  $(V_{sp}/V_0) = \exp\{\beta/[(1-\beta)B'_0]\}$ , with the ratio  $(V_{sp}/V_0)$  obtained from the H11 EOS, the average value is about 0.66. Similar inconsistencies and discrepancies are obtained from the model of Vinet *et al.* but, as we have already pointed out, within the frame of our model, these values of  $\beta$  are inadequate to represent the temperature dependence of the EOS of solids.<sup>9</sup> We found that  $\beta$  changes slightly for different substances and depends on temperature.

Therefore a detailed study of this dependence would permit us to introduce some improvements to our universal EOS, although general features described here should be indeed valid. Further study of this issue is now under investigation.

#### ACKNOWLEDGMENTS

This work was supported by CICYT under research project No. PB92-0553. One of us (M.T.) acknowledges financial support from the Ministerio de Educación y Ciencia (Spain).

- <sup>1</sup>P. Vinet, J. Ferrante, J. R. Smith, and J. H. Rose, *J. Phys. C* **19**, L467 (1986).
- <sup>2</sup>B. W. Dodson, *Phys. Rev. B* **35**, 2619 (1987).
- <sup>3</sup>G. Parsafar and E. A. Mason, *Phys. Rev. B* **49**, 3049 (1994).
- <sup>4</sup>O. Schulte and W. B. Holzapfel, *Phys. Rev. B* **48**, 767 (1993).
- <sup>5</sup>W. B. Holzapfel, *Europhys. Lett.* **16**, 67 (1991).
- <sup>6</sup>P. Vinet, J. R. Smith, J. Ferrante, and J. H. Rose, *Phys. Rev. B* **35**, 1945 (1987).
- <sup>7</sup>J. L. Tallon, *J. Phys. Chem. Solids* **41**, 837 (1980).
- <sup>8</sup>V. G. Baonza, M. Cáceres, and J. Núñez, *Phys. Rev. B* **51**, 28 (1995).
- <sup>9</sup>V. G. Baonza, M. Taravillo, M. Cáceres, and J. Núñez, *Phys. Rev. B* **53**, 5252 (1996).
- <sup>10</sup>V. G. Baonza, M. Cáceres, and J. Núñez, *Chem. Phys. Lett.* **228**, 137 (1994); *J. Phys. Chem.* **98**, 4955 (1994).
- <sup>11</sup>M. Taravillo, V. G. Baonza, M. Cáceres, and J. Núñez (unpublished).
- <sup>12</sup>M. Ross and D. A. Young, *Annu. Rev. Phys. Chem.* **44**, 61 (1993).
- <sup>13</sup>S. Eliezer, A. Ghatak, and H. Hora, *An Introduction to Equations of State: Theory and Applications* (Cambridge University Press, Cambridge, 1988), Chaps. 10 and 12.
- <sup>14</sup>P. Bolsaitis and I. L. Spain, in *High Pressure Technology*, edited by I. L. Spain and J. Paauwe (Dekker, New York, 1977), Vol. I, Chap. 13.
- <sup>15</sup>A. Jayaraman, *Rev. Mod. Phys.* **55**, 65 (1983).
- <sup>16</sup>D. L. Decker, *J. Appl. Phys.* **42**, 3239 (1971).
- <sup>17</sup>H. K. Mao, P. M. Bell, J. W. Shaner, and D. J. Steinberg, *J. Appl. Phys.* **49**, 3276 (1978).
- <sup>18</sup>M. S. Anderson and C. A. Swenson, *J. Phys. Chem. Solids* **36**, 145 (1975).
- <sup>19</sup>S. K. Sikka, *Phys. Lett. A* **135**, 129 (1989); *Phys. Rev. B* **38**, 8463 (1988).
- <sup>20</sup>N. C. Holmes, J. A. Moriarty, G. R. Gathers, and W. J. Nellis, *J. Appl. Phys.* **66**, 2962 (1989).
- <sup>21</sup>W. A. Bassett, T. Takakashi, H. K. Mao, and J. S. Weaver, *J. Appl. Phys.* **39**, 319 (1968).
- <sup>22</sup>J. S. Dugdale and D. K. C. McDonald, *Phys. Rev.* **89**, 832 (1953).
- <sup>23</sup>R. Boehler, I. C. Getting, and G. C. Kennedy, *J. Phys. Chem. Solids* **38**, 233 (1977).
- <sup>24</sup>M. Ross, H. K. Mao, P. M. Bell, and J. A. Xu, *J. Chem. Phys.* **85**, 1028 (1986).
- <sup>25</sup>R. J. Hemley, A. P. Jephcoat, H. K. Mao, C. S. Zha, L. W. Finger, and D. E. Cox, *Nature (London)* **330**, 737 (1987).
- <sup>26</sup>Y. Fei, H. K. Mao, and R. J. Hemley, *J. Chem. Phys.* **99**, 5369 (1993).
- <sup>27</sup>R. Boehler and G. C. Kennedy, *J. Phys. Chem. Solids* **41**, 517 (1980).
- <sup>28</sup>L. C. Chhabildas and A. L. Ruoff, *J. Appl. Phys.* **47**, 4182 (1976).
- <sup>29</sup>R. Boehler and G. C. Kennedy, *J. Phys. Chem. Solids* **41**, 1019 (1980).
- <sup>30</sup>D. L. Decker and T. G. Worlton, *J. Appl. Phys.* **43**, 4799 (1972).
- <sup>31</sup>I. L. Spain, in *High Pressure Technology*, edited by I. L. Spain and J. Paauwe (Dekker, New York, 1977), Vol. I, Chap. 11.
- <sup>32</sup>M. Pagannone and H. G. Drickamer, *J. Chem. Phys.* **43**, 2266 (1965).
- <sup>33</sup>E. A. Perez-Albuerne and H. G. Drickamer, *J. Chem. Phys.* **43**, 1381 (1965).
- <sup>34</sup>T. Yagi, *J. Phys. Chem. Solids* **39**, 563 (1978).
- <sup>35</sup>S. N. Vaidya and G. C. Kennedy, *J. Phys. Chem. Solids* **32**, 951 (1971).
- <sup>36</sup>G. R. Barsch and Z. P. Chang, in *Accurate Characterization the High-Pressure Environment*, edited by E. C. Lloyd (U.S. GPO, Washington, D.C., 1971), p. 173.
- <sup>37</sup>R. G. Greene, H. Luo, and A. L. Ruoff, *Phys. Rev. Lett.* **73**, 2075 (1994).
- <sup>38</sup>W. J. Nellis, J. A. Moriarty, A. C. Mitchell, M. Ross, R. G. Dandrea, N. W. Ashcroft, N. C. Holmes, and G. R. Gathers, *Phys. Rev. Lett.* **60**, 1414 (1988).
- <sup>39</sup>D. L. Heinz and R. Jeanloz, *J. Appl. Phys.* **55**, 885 (1984).
- <sup>40</sup>O. L. Anderson, D. G. Isaak, and S. Yamamoto, *J. Appl. Phys.* **65**, 1534 (1989).
- <sup>41</sup>A. H. Fuchs, Ph. Pruzan, and L. Ter Minassian, *J. Phys. Chem. Solids* **40**, 369 (1979). L. Ter Minassian and Ph. Pruzan, *J. Chem. Thermodyn.* **9**, 375 (1977).
- <sup>42</sup>V. G. Baonza, M. Cáceres, and J. Núñez, *Chem. Phys. Lett.* **216**, 579 (1993).
- <sup>43</sup>H. Spetzler, C. G. Sammis, and R. J. O'Connell, *J. Phys. Chem. Solids* **33**, 1727 (1972).
- <sup>44</sup>S. Bijanki and R. J. Hardy, *J. Appl. Phys.* **49**, 215 (1978).
- <sup>45</sup>C. R. Tilford and C. A. Swenson, *Phys. Rev. B* **5**, 719 (1972).
- <sup>46</sup>C. Kittel, *Introduction to Solid State Physics*, 4th ed. (Wiley, New York, 1971).
- <sup>47</sup>G. R. Barsch and Z. P. Chang, *Phys. Status Solidi* **19**, 139 (1967).
- <sup>48</sup>J. T. Lewis, A. Lehoczky, and C. V. Briscoe, *Phys. Rev.* **161**, 877 (1967).
- <sup>49</sup>O. G. Peterson, D. N. Batchelder, and R. O. Simmons, *Phys. Rev.* **150**, 703 (1966).
- <sup>50</sup>D. L. Losee and R. O. Simmons, *Phys. Rev.* **172**, 944 (1968).
- <sup>51</sup>A. C. Bailey and B. Yates, *Philos. Mag.* **16**, 1241 (1967).
- <sup>52</sup>J. E. Rapp and H. D. Merchant, *J. Appl. Phys.* **44**, 3919 (1973).